INTL JOURNAL OF ELECTRONICS AND TELECOMMUNICATIONS, 2023, VOL. 69, NO. 3, PP. 579-586
Manuscript received May 8, 2023; revised July, 2023. DOI: 10.24425/ijet.2023.146510

Development of Methodological, Hardware, and Software of the Incoherent Scatter Radar of Institute of Ionosphere (Kharkiv, Ukraine)

Leonid Emelyanov, and Artem Miroshnikov

***Abstract*—We present the met determinate hodological features and new subsystem for receiving, digitizing and processing signals at the intermediate frequency of the incoherent scatter (IS) radar. The implemented method, subsystem and flexible software made it possible to avoid the influence of a number of instrumental factors on the accuracy of determining the quadrature components of the IS signal correlation function used to determine the ionospheric parameters, to adapt the digital filtering parameters, the value of the correlation delay step and the number of ordinates of the measured correlation function to IS signals from different altitudes and under different space weather conditions, to effectively test radar systems for the subsequent taking into account hardware factors and, thus, to improve the accuracy of the measured ionospheric parameters. The experimental results are presented.**

***Keywords*—incoherent scatter radar; incoherent scatter signal; signal reception and processing; ionospheric plasma parameters**

I. Introduction

THE incoherent scatter (IS) technique is the most informative method for studying the ionosphere. It allows to determinine simultaneously a number of parameters of the ionosphere in a wide range of altitudes with sufficient height resolution [1, 2]. This method includes sounding the ionosphere with a powerful signal, receiving a weak signal incoherently scattered by the ionospheric plasma, and signal processing.

Large-sized antennas, powerful radio transmitting and sensitive radio receiving devices are used to determine the parameters of the ionosphere by the IS method [1–10]. Improvement of the equipment, methods of measurements, as well as data processing algorithms has been carried out at the existing IS radars in the world and is relevant at the present time [6–10]. The IS radar of Institute of Ionosphere [11] is also being improved in accordance with the development of the principles of distributed targets radiolocation, the electronic components and computer technology.

The IS radar of Institute of Ionosphere that is located near Kharkiv, Ukraine (49.67° N, 36.29° E) has the follows main parameters. The operating frequency is 158 MHz. The effective aperture of the 100-meter zenith-directed Cassegrain antenna is about 3700 m^2. The transmitter peak pulse power is normally 2 MW. The pulse repetition frequency is 24.4 Hz. The polarization of sounding signal is mostly circular. The effective noise temperature of the receiver is 120 K.

The ionospheric parameters (electron density, electron and ion temperatures, plasma drift velocity, ion composition etc.) are determined from the quadrature components of the measured correlation function (CF) of the IS signals extracted in the low frequency region by two quadrature receiver channels using synchronous detection.

The processing of the IS signal at an intermediate frequency (IF) has advantages in some cases. It allows us to use algorithms that are adapted to the height range under study and the state of the ionosphere, as well as improve the accuracy of measurement of the IS signal parameters (and, accordingly, the ionosphere parameters), excluding the influence of a number of instrumental factors and increasing the number of discrete samples of the signal for its digital processing.

The purpose of this work is to improve the methodology of IS signal reception, digitization and processing, implement a subsystem that allows to process signals using records of digitized signal values at the IF with an increased sampling rate, as well as design processing algorithms adapted to the IS signal parameters that depend on the state of the ionosphere.

II. Existing System of Kharkiv Radar for Receiving and Processing the IS Signal at a Low Frequency

To obtain data on the ionosphere parameters using the IS radar of Institute of Ionosphere, a highly sensitive radio receiver with triple frequency conversion is used and correlation processing of the signals extracted by the quadrature channels of the receiver is performed using synchronous detection and signal filtering [11].

The block diagram of the existing system for receiving and processing the IS signal at a low frequency is shown at the top of Figure 1. In the RF section, the radio transmitter pulse leaking from the antenna-feeder system is blanked in order to suppress it during sounding. In the IF section, the spectrum of the IS signal is transferred from the carrier frequency f_0 = 158 MHz to the IF f_{if} = 972.4 kHz. Each of the two quadrature channels contains a synchronous detector (with a low-pass filter and amplifier) and an analog-to-digital converter (ADC). The heterodyne signals with frequencies f_{lo1}, f_{lo2} and f_{slo} are formed in such a way that the center frequency of the spectrum of the IS signal at the output of the IF section (f_{if}) is equal to the frequency of the synchronous heterodyne f_{slo}. in the absence of a Doppler shift caused by the movement of the ionospheric plasma. Phase shifter with a phase difference φ=90° is used for the formation of quadrature signals.

Strict requirements are imposed on this system to ensure the identity of the parameters of the quadrature channels, the

Leonid Emelyanov and Artem Miroshnikov are with Institute of Ionosphere of NAS and MES of Ukraine (e-mail: leonid.ya.emelyanov@gmail.com, moneytu@gmail.com).

accuracy and stability of the formation of quadrature signals for measuring the ionospheric plasma drift velocity.

III. Hardware and Methodological Implementation of Measuring the Parameters of the IS Signal at the Intermediate Frequency

A new method was proposed, which provides for the processing of the received signal directly at the IF of the radio receiver [12]. In this case, the quadrature components of the received signal CF are determined exclusively by software, which allows avoiding errors caused by the possible non-identity of the two channels of the analog path of the receiver and two ADCs of the signal processing system. It also eliminates the need to control and maintain a phase difference of 90° of the synchronous heterodyne signals generated using an analog phase shifter.

In addition, it becomes possible to significantly increase the sampling frequency of discrete samples of the processed signal to improve the accuracy of measuring the parameters of the IS signal. Modern high-performance computers allow recording and storing a large array of signal samples at the IF, as well as using digital processing with optimized algorithms (specific for different ranges of heights and state of the ionosphere).

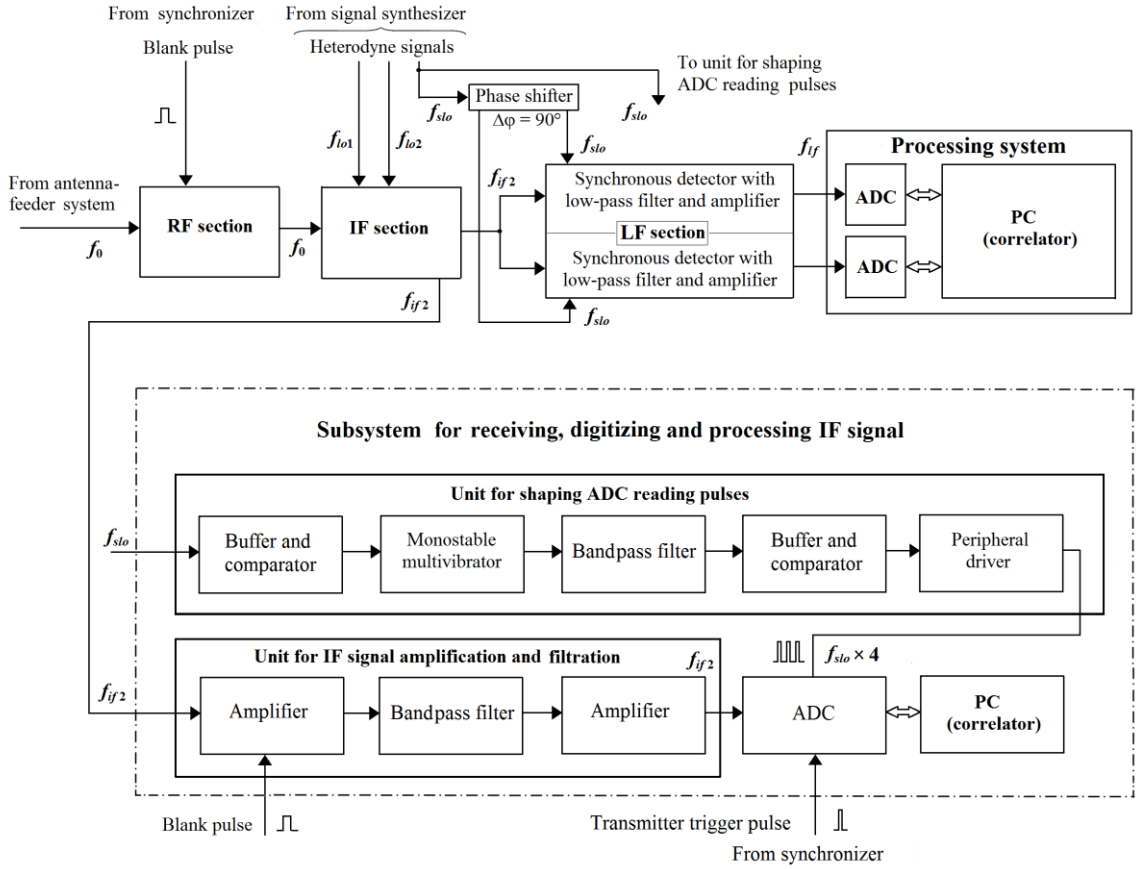

Fig. 1. Block diagram of a system for receiving and processing a signal as part of the IS radar

Figure 1 shows a block diagram of a subsystem for receiving, digitizing and processing a signal at the IF, which uses only one high-speed ADC based on the L-card E20-10 module (https://www.manualslib.com/download/1614583/L-Card-E20-10.html). The subsystem supplements the existing radio receiving system. The subsystem includes the unit for IF signal amplification and filtration (consisting of two amplifiers and a bandpass filter), the ADC, the personal computer (PC), and the unit for shaping ADC reading pulses.

For rigid binding of the ADC reading pulses to the IF, the signal of synchronous heterodyne with a frequency $f_{slo} = f_{if} = 972.4$ kHz is used as an input signal for the unit for shaping ADC reading pulses. This ensures coherent operation of the radio receiver and radio transmitter, to which the signals of heterodynes and the master signal from the synthesizer are supplied, respectively, and excludes the error described in [13] when one of the two data streams is not synchronized with the other one. At the output of the unit, pulses are formed with a repetition rate equal to $4f_{slo}$, i.e. with a repetition period equal to a quarter of the period of the synchronous heterodyne signal. Thus, adjacent signal samples are in quadrature dependence. This makes it possible to determine the ordinates of the quadrature components of the CF $R(\tau)$ with time lags (arguments) τ that are multiples of the IF signal period and are optimal for specific conditions.

The transmitter trigger pulses are used as a signal to indicate the start of each radar scan.

Special requirements are imposed on stability (temperature and time) and frequency multiplication accuracy for the unit for shaping ADC reading pulses. This is due to the precision of the signal sampling to ensure the quadrature of its samples, which are used for further calculation of the IS signal parameters and the ionosphere parameters. Several variants of frequency multipliers were analyzed and the most acceptable variant was

chosen to generate a pulse signal with a quadruple IF [12]. This variant based on the selection of the 4th harmonic from a sequence of pulses with an optimal ratio of repetition period and duration.

IV. Processing of Intermediate Frequency Signal

During the measurement of ionospheric parameters, digitized instantaneous values (discrete samples) of the receiver output signal are recorded and stored in binary files, each of which, as a rule, corresponds to a one-minute measurement session. These files also contain service information [14].

Figure 2 shows an example of one of the experimentally obtained radar scans with the measured discrete samples of the IF signal at the output of the radio receiver. There are 1464 scans during each one-minute measurement session, and each scan contains 85552 signal samples. The abscissa shows the height values in kilometers, and the ordinate shows the signal voltage values in relative units. The height reading starts from the middle of the sounding pulse (see on the left side of the figure, where the transmitter pulse seeping through the antenna switch of the feeder path and the blanking elements of the receiver is visible). In the scan sections on the left, the IS signal is visible against the background of space and instrumental noise.

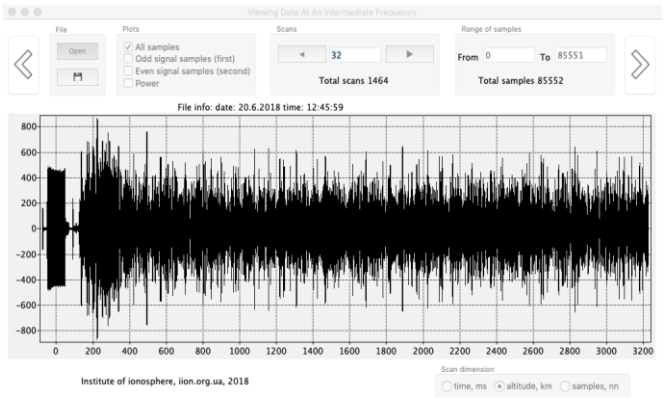

Fig. 2. Experimental data obtained during the measurement of ionospheric parameters: digitized and recorded IF signal at the output of the radio receiver during one radar scan

The processing of the received signal at the IF includes the same stages as the signal processing at a low frequency described in [15, 16]: estimation of CF ordinates, data review and removal of clutter (reflection signals from flying objects), time averaging (usually 15 min), noise exception, taking into account the antenna switch recovery characteristic, estimation of the ionospheric plasma parameters.

The features of the method of correlation processing at the IF proposed by us can be easily represented using Figure 3, which illustrates the CFs of the IS signal at the IF in the absence of the signal spectrum Doppler shift (solid lines) and in its presence (dashed line) caused by the general movement of the plasma along the radar beam. The dots show the CF ordinates involved in the correlation processing. $R_o(\tau)$ is the CF envelope.

Subject to the relation $T=T_{slo}/4$, the ordinates of the sine component of the CF corresponding to the ordinates of the measured CF with a fixed time lag (τ_k-T) or (τ_k+T) are equal to zero in the absence of plasma motion (Doppler shift of the spectrum of the IS signal $f_d=0$) and differ from zero when $f_d \neq 0$, and the cosine component $R(\tau)=R(\tau_k)$ is equal to the CF envelope $R_o(\tau_k)$ in the first case and is close to it in the second case. The use of two ordinates of the sine component for each k-th CF argument makes it possible to eliminate the bias in determining the velocity of the ionospheric plasma.

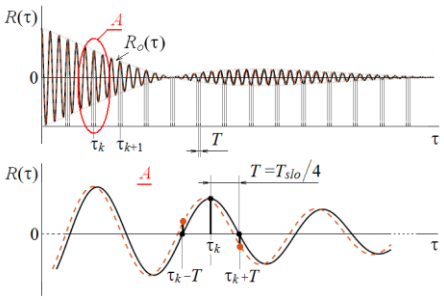

Fig. 3. Correlation functions of the IS signal at the intermediate frequency in the absence of a Doppler shift of the spectrum (solid lines) and in its presence (dashed lines) caused by plasma motion along the radar beam

Correlation processing of the IF signal includes the following.

The ordinates of the cosine and sine components of the CF of the received signal are estimated for each discrete radar time delay t_j, corresponding to the altitude $h_j=ct_j/2$ of the center of the scattering section of the ionospheric plasma with the length $\Delta h_j=c\tau_{si}/2$, for fixed correlation time lags (CF arguments) τ_k.

$$R_{\cos(s+n)}(h_j,\tau_k)=\overline{u(t_j)\,u(t_j+\tau_k)},$$

$$R_{\sin(s+n)}(h_j,\tau_k+T)=\overline{u(t_j)\,u(t_j+\tau_k+T)},$$

$$R_{\sin(s+n)}(h_j,\tau_k-T)=\overline{u(t_j)\,u(t_j+\tau_k-T)},$$

where $u(t_j)$ are instantaneous signal values at the time points t_j, c is the speed of light, $\tau_k=k\Delta\tau$, k is CF ordinate number, $k=0, 1,\ldots,n$, n is a quantity of CF ordinates used for calculation of ionospheric parameters, $\Delta\tau$ is a correlation lag step (CF argument step), $T=T_{slo}/4$, τ_{si} is sounding pulse duration.

The CFs of the IS signal are determined as the difference between the CF of the signal + noise mixture in each specific area of the radar scan and the CF of the noise averaged over the scan sections where the IS signal is absent:

$$R_{\cos}(h_j,\tau_k)=R_{\cos(s+n)}(h_j,\tau_k)-\overline{R_{\cos(n)}(\tau_k)},$$

$$R_{\sin}(h_j,\tau_k\pm T)=R_{\sin(s+n)}(h_j,\tau_k\pm T)-\overline{R_{\sin(n)}(\tau_k\pm T)},$$

$$R_{\sin}(h_j,\tau_k)=\frac{1}{2}\left[R_{\sin}(h_j,\tau_k-T)-R_{\sin}(h_j,\tau_k+T)\right].$$

The ordinates of the CF envelope are defined as

$$R_o(h_j,\tau_k)=\sqrt{R^2_{\cos}(h_j,\tau_k)+R^2_{\sin}(h_j,\tau_k)}.$$

Normalized CFs

$$r_o(h_j,\tau_k)=R_o(h_j,\tau_k)/R_o(h_j,0)$$

are used to calculate the altitude profiles of ionospheric parameters (ion (T_i) and electron (T_e) temperatures and ion composition) by comparing measured CFs with library of theoretical CFs using the least squares method [16, 17].

To determine the electron density N_e, the normalized electron density profile is calculated [17]:

$$N_e(h_j)_{norm} = \frac{q(h_j)h_j^2\left[1+\frac{T_e(h_j)}{T_i(h_j)}\right]}{\left\{q(h_j)h_j^2\left[1+\frac{T_e(h_j)}{T_i(h_j)}\right]\right\}_{\max}},$$

where $q(h_j)$ is the ratio of IS signal power to noise power, $q(h_j)=R(h_j,0)/R_n(h_j,0)$. The absolute values of $N_e(h_j)$ (in m^{-3}) are determined by linking the $N_e(h_j)_{norm}$ profile at the maximum to the critical frequency f_oF2 (in MHz) measured by the ionosonde:

$$N_e(h_j)=1.24\cdot10^{10}N_e(h_j)_{norm}(f_o\mathrm{F2})^2.$$

The ionospheric plasma drift velocity is calculated by the formula

$$V_z(h_j)=-\frac{\lambda}{4\pi n}\sum_{k=1}^{n}\frac{1}{\tau_k}\left[\operatorname{arctg}\frac{R_{\sin}(h_j,\tau_k)}{R_{\cos}(h_j,\tau_k)}\right].$$

The developed software makes it possible to quickly set the CF lag step $\Delta\tau$ and the number of CF ordinates used for further processing. With a decrease in $\Delta\tau$, the accuracy of determining the parameters of the ionosphere increases. In principle, the $\Delta\tau$ minimum can be equal to the period T of the ADC reading pulses or the period T_{slo} of oscillations of the synchronous heterodyne signal (IF period). However, from a practical point of view (the amount of accumulated information and the possibility of real-time processing during the ionospheric parameter measurements), there is no such need. As calculations show, when using a sounding radio pulse signal with the carrier frequency f_0=158 MHz and duration τ_{imp}=650 μs, the most acceptable values of $\Delta\tau$ to reduce the statistical and systematic errors in determining ionospheric parameters are within $4T_{slo}<\Delta\tau<36T_{slo}$. Moreover, the choice of $\Delta\tau$ depends on the parameters of the ionosphere (ion and electron temperatures, ion composition) for different heights and its state (see, for example, [12, 18]).

Thus, if 18–20 CF ordinates are used in the correlation interval (the second zero of the CF), which is sufficient to determine the parameters of the ionosphere, the optimal step is from $\Delta\tau$=5–10 μs for the heights of the outer ionosphere, where hydrogen ions (H^+) predominate, to $\Delta\tau$=30–40 μs for heights near the peak of the F layer, where oxygen ions (O^+) are mainly present.

V. EXPERIMENTS WITH THE SUBSYSTEM OF RECEIVING, DIGITIZING AND PROCESSING INCOHERENTLY SCATTERED SIGNAL SELECTED AT THE INTERMEDIATE FREQUENCY

After the development, manufacture and adjustment of the subsystem for receiving, digitizing and processing the signal at the IF, it was introduced into the radio receiver of the IS radar, and experiments were conducted.

Figures 4–6 show the measurement data obtained on 20 June 2018 with a 15-minute accumulation (12:30–12:45 EEST).

The measured normalized CF of the IS signal scattered at a height of 280 km is shown in Figure 4.

In the calculation of this CF, all signal samples and the minimum possible correlation lag step $\Delta\tau=T=T_{slo}/4$=0.257 μs were used. In this case, the calculated value of the vertical component of the plasma drift velocity is V_z= –62 m/s.

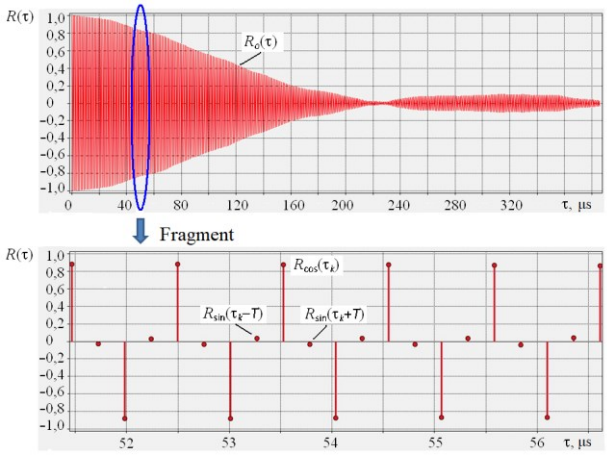

Fig. 4. Correlation function of the IS signal from the height of 280 km (correlation lag step $\Delta\tau=T=T_{slo}/4$=0.257 μs)

Figure 5 shows the measured quadrature components of the IS signal for three heights of the ionosphere.

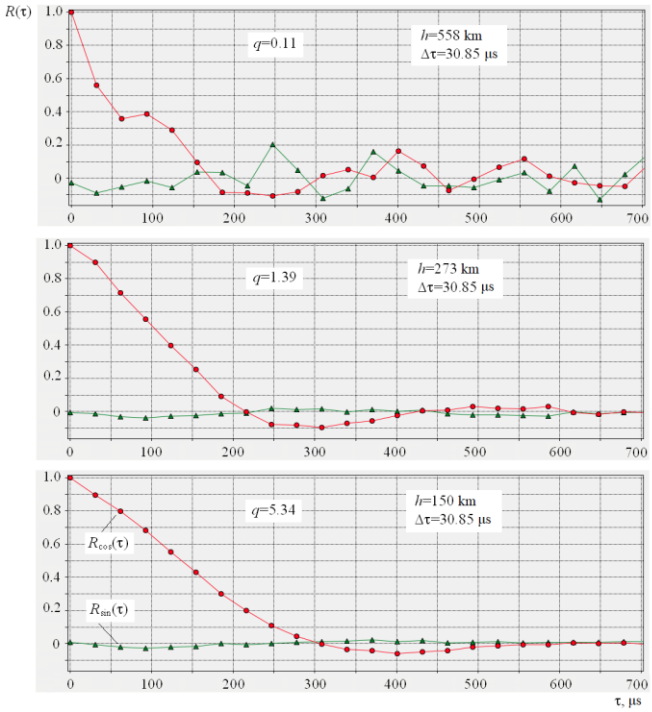

Fig. 5. Estimates of the cosine and sine components of the correlation function of the IS signal for three heights: 150, 273 and 558 km (step $\Delta\tau=120\cdot T\approx30.85$ μs, q is the signal-to-noise ratio)

It can be seen from the figure that the correlation interval decreases with increasing height. For low and medium heights, the number of CF ordinates is sufficient for further calculations, and the choice of such a step $\Delta\tau$ is justified. For the upper ionosphere, the number of CF ordinates can be insufficient to determine the parameters of the ionosphere with acceptable

accuracy (especially at night, when the correlation interval can be extremely short).

The ratio of the power of the signal scattered at high altitudes to the noise power ($q=P_s/P_n$) decreases with increasing altitude, and the resulting increase in the statistical error can to some extent be compensated for by a decrease in the step $\Delta\tau$ and, therefore, by an increase in the number of CF ordinates that have physical meaning and participate in processing.

To illustrate the above, Figure 6 shows a comparison of the results of correlation processing using the adaptive mode of a shorter CF lag step (in this case, $\Delta\tau=40\cdot T_1=10.284$ μs) and the mode with a standard (until now) step $\Delta\tau=T_2\approx30$ μs. T_1 and T_2 are signal sampling intervals.

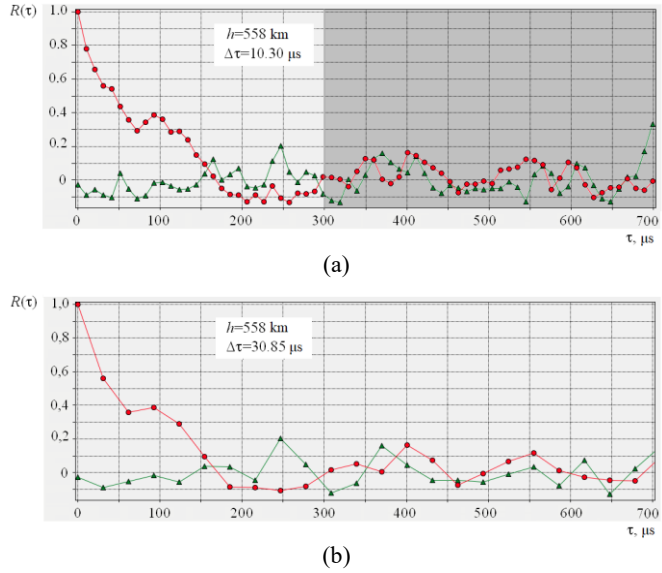

Fig. 6. Comparison of the results of correlation processing when using adaptive (a) and conventional (b) modes

From Figure 6, you can see that when using the adaptive mode ($\Delta\tau\approx10.3$ μs), the CF of the signal scattered in the upper ionosphere can be determined more accurately even for daytime.

Another advantage is that the ordinates in the CF tail, which are useless for processing (in this case, shown in the darkened section of Figure 6a for $\tau > 300$ μs), are not used in further calculations of the ionospheric parameters, thereby no additional error due to the statistical spread of values of these ordinates is introduced, PC memory saves and processing time reduces.

Calculations showed that the standard deviation of the CF, when comparing it with the model CF, decreased approximately 2 times when using the step $\Delta\tau=40\cdot T\approx10.3$ μs instead of $\Delta\tau = 80\cdot T \approx 20.6$ μs and 2.5 times instead of $\Delta\tau = 120\cdot T \approx 30.9$ μs.

VI. TESTING OF THE SUBSYSTEM FOR RECEIVING, DIGITIZING AND PROCESSING THE SIGNAL AT THE INTERMEDIATE FREQUENCY AND OTHER SYSTEMS OF THE IS RADAR

To test the structural units of the receiving-processing path and the IS radar as a whole, the principles of generating signals for testing and monitoring the IS radar given in [19] were used.

Measurements of the ionospheric plasma velocity are the most sensitive, which is associated with the need to determine the Doppler shift of the IS signal spectrum, which is 2–4 orders of magnitude smaller than the width of this spectrum. Testing of a parameter equivalent to the measured velocity of ionospheric plasma drift has been carried out. Figure 7 shows the result of one of the testing sessions for measuring the velocity V_d by a harmonic signal supplied to the path of the 2nd IF. In this case, the frequency shift of the testing signal relative to the 2nd IF ($f_{if2}=f_{slo}$ = 972375.4 Hz), simulating the Doppler shift, is equal to 124.2 Hz, which corresponds to the velocity of –117.827 m/s.

Testing with different values of the simulated velocity showed that the absolute error in determining the velocity does not exceed 0.05 m/s, and the standard deviation (RMS) is about 0.1 m/s. This is much less than the root-mean-square error in determining the plasma drift velocity in real measurements with the IS signal that is random and is received against the background of space and instrumental noise. With a temporal accumulation of 15 minutes, it usually varies from 1 m/s at ionospheric heights close to the F2 peak height, to 20–30 m/s at great heights of the outer ionosphere, where the signal-to-noise ratio is $q<<1$.

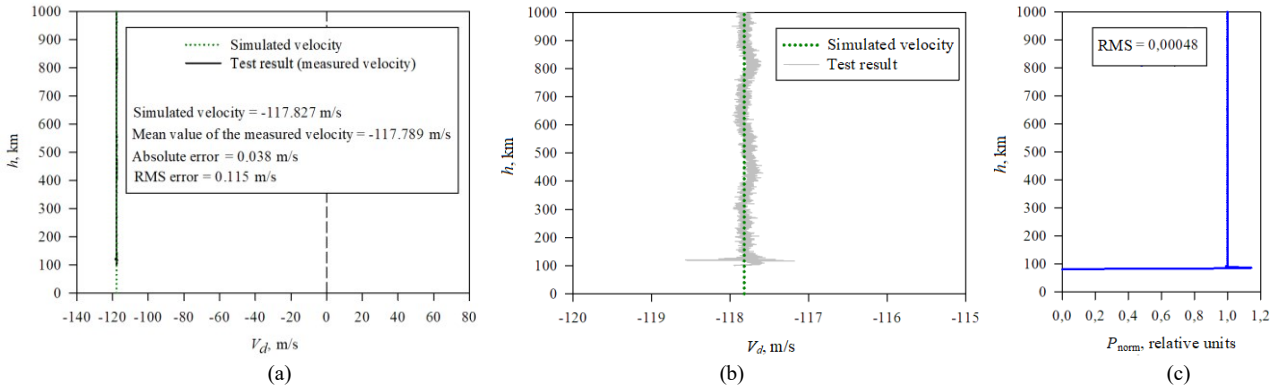

Fig. 7. The result of testing the plasma drift velocity ((a) and (b) in different scales) and (c) the stability of the transmission gain of the receiving-digizing path (distribution of signal power over the radar scan

Based on the same measurements of the power, CFs of the signal at the output of the IF path, and the parameter-analogue of the ionospheric plasma drift velocity when the transmitter is inoperative, it was found that blanking the receiver does not affect the stability of its transmission gain and tuning frequency during the radar scan.

The recovery characteristic of the antenna switch with the gas-discharge arresters was measured throughout the radar scan

(normalized power transfer coefficient of the receiving path), which is used to correct data in the signal processing. To do this, with the transmitter operating, a harmonic test signal from a highly stable in frequency generator was fed through a monitoring antenna via a radio channel to the radar antenna and then through a feeder path with antenna switch to the input of the receiver system. The measurement result is shown in Figure 8.

It can be seen that, as a result of testing, the measured value of the velocity is close to the value of the simulated velocity.

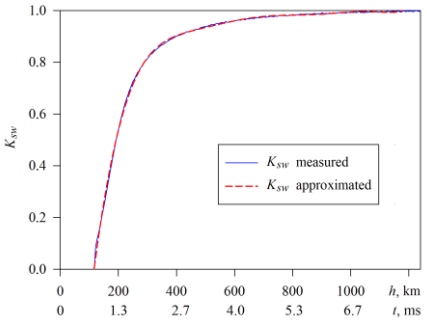

Fig. 8. Measured and approximated characteristics of antenna switch

The recovery characteristic of the antenna switch was approximated by the least squares method by the polynomial $K_{\text{discharge}}=a_0+a_1h+a_2h^2+a_3h^3+a_4h^4+a_5h^5+a_6h^6+a_7h^7+a_8h^8$, were $a_0=1.28$, $a_1=1.25\cdot10^{-2}$, $a_2=2.46\cdot10^{-6}$, $a_3=-1.96\cdot10^{-7}$, $a_4=6.77\cdot10^{-10}$, $a_5=-1.11\cdot10^{-12}$, $a_6=9.95\cdot10^{-16}$, $a_7=-4.66\cdot10^{-19}$, $a_8=8.95\cdot10^{-23}$. The approximated characteristic shown by the dashed line in Figure 8 uses in processing.

The characteristic measured with a minimum height step Δh=0.039 km (which corresponds to a time step Δt_j=0.26 μs) practically coincides with characteristic measured with Δh=4.62 km Δt_j=30.85 μs, that shown in Figure 8.

Correction of the IS signal CF for the given lag τ_k and height $h_j=ct_j/2$ is carried out according to the formula [16, 17]

$$R^*(h_j,\tau_k)=R^*(t_j,\tau_k)=\frac{R(t_j,\tau_k)}{\sqrt{K_{sw}(t_j)K_{sw}(t_j+\tau_k)}}.$$

Here $K_{sw}(t)$ is the recovery characteristic of antenna switch.

The IS radar altitude scale is periodically calibrated by measuring the parameters of reflection signals from cataloged man-made space objects that fell into the main lobe of the antenna pattern.

An example of one of radar scans with reflection from a space object is shown in Figure 9. According to the "North American Aerospace Defense Command" satellite data catalog (http://www.celestrak.com/NORAD/elements/starlink.txt), the exact time of flight of the STARLINK-1511 satellite above the Kharkiv IS radar (49.6763° N, 36.2922° E) in 16 June 2021 was 14:21:23 with flight parameters: 157.1° elevation, 88.2° azimuth, 552 km altitude.

Zero height (zero of the time scale of the radar scan) corresponds to the middle of the sounding pulse; similarly, the middle of the reflected signal corresponds to the known height of the cataloged space objects.

Testing shows that the altitude on the IS radar altitude scale corresponds to the altitude of the space object. A similar result was obtained for other cataloged objects. That is, the altitude scale is quite accurate (the error in determining the height does not exceed 0.077 km, which corresponds to the IF signal sampling step ($T=T_{slo}/4=0.257$ μs).

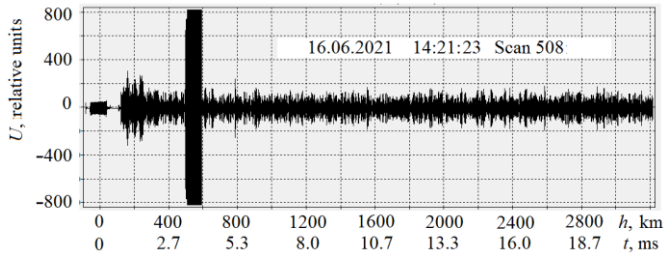

Fig. 9. Fragment of the radar scan digitized at the intermediate frequency with the reflected signal from the STARLINK-1511 space object

Owing to the subsystem for receiving, digitizing and processing the signal at the IF, it became possible to measure the distribution of the amplitude and carrier frequency of the sounding radio pulse along its length. These parameters can be taken into account when processing the IS signal. This is especially important for precision measurements of the ionospheric plasma velocity.

For experimental measurements of the parameters of the sounding signal, its reception is carried out using a test antenna, undistorted signal passage in the individual receiving path is ensured due to exclusion the antenna switch and sufficient attenuation of the signal at the receiver input.

To calculate the signal amplitude for the current sample u_j, 4 adjacent samples are sufficient, interconnected by a quadrature dependence $U_m=\sqrt{1/2\left(u_{j-1}^2+u_j^2+u_{j+1}^2+u_{j+2}^2\right)}$. To eliminate the bias, we used the expression

$$U_{mj}=\frac{1}{2\sqrt{2}}\left[\sqrt{\left(u_{j-2}^2+u_{j-1}^2+u_j^2+u_{j+1}^2\right)}+\sqrt{\left(u_{j-1}^2+u_j^2+u_{j+1}^2+u_{j+2}^2\right)}\right].$$

The carrier frequency of the sounding signal in the region of each sample was determined from the expression we obtained

$$\Delta f(t_j)=\Delta f_j=\frac{f_{slo}}{2\pi n}\left(\arcsin\frac{u_{(j+4n)}}{U_{m(j+4n)}}-\arcsin\frac{u_j}{U_{mj}}\right),$$

where t_j is the sampling time on the radar scan, $t_j=j/4f_{slo}$, n is the number of fill signal periods between two samples to be compared. Simulation of the calculation of U_{mj} and Δf_j with using a harmonic signal and different initial Δf and n showed high calculation accuracy (the Δf error does not exceed 0.064 Hz for Δf within –200…+200 Hz and does not exceed 0.004 Hz when $-50<\Delta f<+50$ Hz).

As an example, the sounding signal parameters measured during the checkout of the IS radar are shown in Figure 10.

It can be seen that the restoration of the sounding signal amplitude in this case took place for about 0.25 ms. On the average, the difference between the carrier frequency and the radar operating frequency f_0 in this case Δf_{aver} =53.8 Hz, which corresponds to $3.4\cdot10^{-7}$ %. Despite the very small value of Δf_{aver} compared to f_0, it is commensurate with the Doppler shifts of the spectrum of the IS signal during ionospheric measurements of the plasma velocity. To eliminate the measurement error of the velocity V_d, a correction is required $\Delta V_d=-\Delta f_{aver}\lambda/2$ (in this case, the radar wavelength λ=1.9 m and ΔV_d=51.1 m/s).

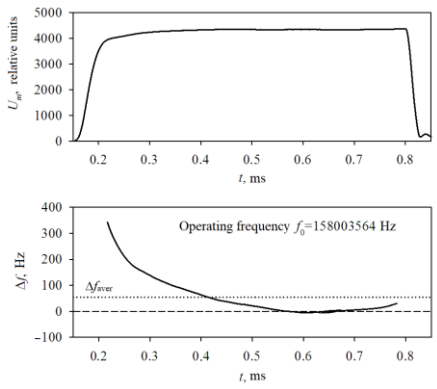

Fig. 10. Variations of the sounding pulse parameters along its length: amplitude (U_m) and deviation (Δf) of the carrier frequency relative to the radar operating frequency

The same results were obtained by an independent method for determining Δf, Δf_{aver} and, accordingly, the value of the velocity correction ΔV_d using the correlation processing of the sounding radio pulse, similar to the processing of the IS signal. The calculation differs in the choice of the number of ordinates involved in processing and the lag step (argument) of the CF τ_k. As the analysis showed, in this case (of a deterministic signal with a finite duration) it was expedient and sufficient to use one CF ordinate with a lag τ_k =16.45 μs. The calculation involved all samples throughout the sounding pulse with a minimum step equal to Δt_j =0.26 μs. The normalized values of the voltage envelope of the sounding radio pulse were determined from the measured power values (CF with a lag equal to zero).

VII. EXPERIMENTAL RESULTS OF IONOSPHERIC PARAMETERS MEASUREMENTS

Figure 11 shows, as an example, seasonal the height profiles of electron density (a), electron and ion temperatures (b), and plasma drift velocity (c), obtained using the correlation processing of the signal at the IF with a time accumulation of 15 min.

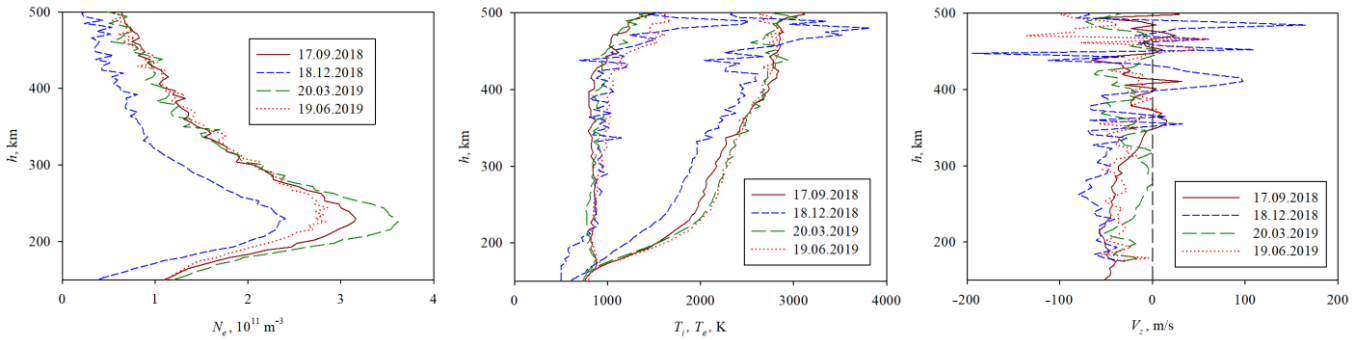

(a) (b) (c)

Fig. 11. Height profiles of electron density (a), electron and ion temperatures (b), and plasma drift velocity (c) for four seasons

It is proposed to further improve the accuracy of the estimation of the IS signal CF and, therefore, the accuracy of the determination of the ionospheric parameters by increasing the signal-to-noise ratio (SNR), using a set of digital filters during signal processing. Bandpass filters with infinite impulse response were created using the SciPy library of the Python. For the analysis, 17-order Chebyshev filters were created with a bandwidth of 10, 14, 19, and 24 kHz and with a linear characteristic in the passband and signal suppression beyond the passband at the level of 60 dB.

Figure 12a shows the height profiles of the SNR of one of the measurement sessions when processed using a series of digital band pass filters. The value of 38 kHz corresponds to the bandwidth of the analog part of the radio receiver (of the bandpass filter of the unit for IF signal amplification and filtration, see Figure 1). As can be seen, the SNR improves significantly with narrowing of the bandwidth, but in some cases, a narrow-band filter can distort the signal spectrum and, as a result, introduce an error into the measured parameters of the ionosphere. Figures 12b, 12c, 12d show that the “10 kHz” filter introduces significant distortions in the measured parameters at altitudes above 400 km. This is caused by an increase in the width of the IS signal spectrum at high altitudes. At altitudes below 300 km, distortions of the $N_e(h)$ profile are more noticeable when using the “38 kHz” and “14 kHz” filters compared to the $N_e(h)$ profile with the “10 kHz” filter, which is explained by an increase in the statistical dispersion of the measured parameters with a decrease in the signal-to-noise ratio, as well as the likely presence of interference over a wider bandwidth. Figure 12e illustrates the solution to the problem by using the most appropriate filters for different height ranges.

VIII. CONCLUSIONS

The developed and implemented method and subsystem for receiving, digitizing and processing signal at an intermediate frequency made it possible to avoid the influence of a number of instrumental factors on the accuracy of determining the quadrature components of the correlation function of the IS signal, to adapt the digital filtering parameters, correlation delay step value and the number of ordinates of the measured correlation function to the IS signals from different altitudes and under different space weather conditions, to effectively test radar systems for subsequent taking into account hardware factors and, thus, to improve the accuracy of the measured ionospheric parameters. Recording a large number of signal samples with small (about 0.26 μs) intervals between them allows you to test and use at any time various processing algorithms that are most suitable for specific geophysical and measurement conditions. The obtained experimental results confirm the effectiveness of the proposed method and the developed subsystem.

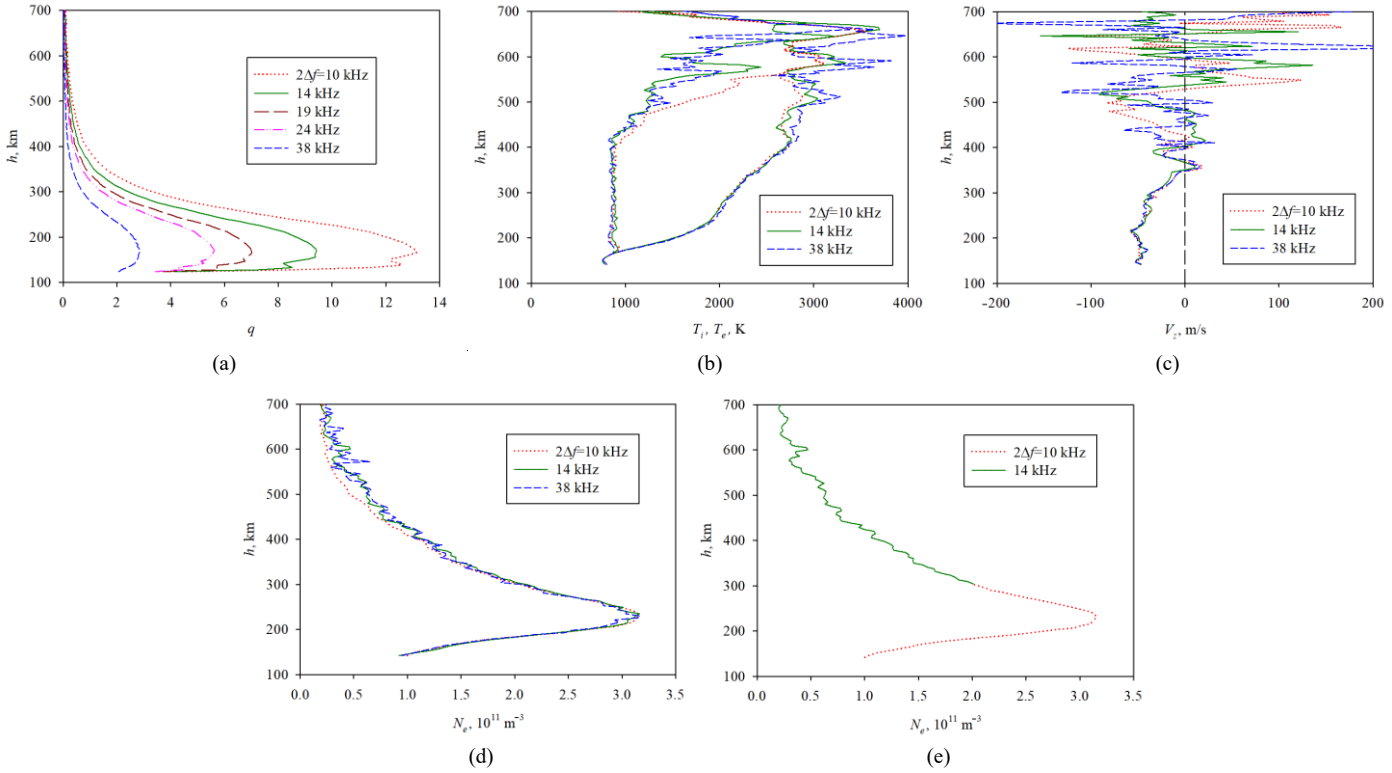

Fig. 12. Height profiles of parameters for a set of digital filters:
signal-to-noise ratio (a), electron and ion temperatures (b), plasma drift velocity (c), electron density (d and e)

REFERENCES

[1] J. V. Evans, "Theory and practice of ionosphere study by Thomson scatter radar" Proceedings of the IEEE, vol. 57, no 4, pp. 496–530, 1969. https://doi.org/10.1109/PROC.1969.7005

[2] J. P. Dougherty and D. T. Farley, "A Theory of Incoherent Scattering of Radio Waves by a Plasma", Proceedings of the Royal Society, vol 259(1296), pp. 79–99, 1960. https://doi.org/10.1098/rspa.1960.0212

[3] R. F. Woodman, D. T. Farley, B. B. Balsley, and M. A. Milla, "The early history of the Jicamarca Radio Observatory and the incoherent scatter technique", Hist. Geo Space. Sci., vol. 10, pp. 245–266, 2019. https://doi.org/10.5194/hgss-10-245-2019

[4] T. Sato, A. Ito, W. L. Oliver, S. Fukao, T. Tsuda, S. Kato, and I. Kimura, "Ionospheric incoherent scatter measurements with the middle and upper ionosphere radar. Techniques and capability", Radio Sci., vol. 24, pp. 85–98, 1989. https://doi.org/10.1029/RS024i001p00085

[5] P. J. S. Williams and G. N. Taylor, "The UK incoherent scatter radar", Radio Sci., vol. 9, no. 2, pp. 85–88, 1974. https://doi.org/10.1029/RS009i002p00085

[6] "EISCAT_3D: A Next-Generation European Radar System for Upper-Atmosphere and Geospace Research" / U.G. Wannberg et al. The Radio Science Bulletin, N 332, pp 75–88, 2010. DOI: 10.23919/URSIRSB.2010.7911050

[7] M. Lehtinen, J. Markkanen, A. Väänänen, A. Huuskonen, B. Damtie, T. Nygrén, J. Rahkola, "A new incoherent scatter technique in the EISCAT Svalbard Radar", Radio Sci., vol. 37, no. 4, 2002. https://doi.org/10.1029/2001RS002518

[8] J. M. Holt, P. J. Erickson, A. M. Gorczyca, and T. Grydeland, "MIDAS-W: a workstation-based incoherent scatter radar data acquisition system", Ann. Geophys, vol. 18, no. 9, pp. 1231–1241, 2000. https://doi.org/10.1007/s00585-000-1231-3

[9] T. Grydeland, F. D. Lind, P. J. Erickson, and J. M. Holt, "Software Radar signal processing", Ann. Geophys., vol. 23, no. 1., pp. 109–121, 2005. https://doi.org/10.5194/angeo-23-109-2005

[10] Z. Ding, J. Wu, Z. Xu, B. Xu, and L. Dai, "The Qujing incoherent scatter radar: system description and preliminary measurements", Earth Planets Space, vol. 70, no. 1, 2018. https://doi.org/10.1186/s40623-018-0859-8

[11] I. F. Domnin, Ya. M. Chepurnyy, L. Ya. Emelyanov, S. V. Chernyaev, A. F. Kononenko, D. V. Kotov, O. V. Bogomaz, and D. A. Iskra, "Kharkiv Incoherent Scatter Facility", Bulletin of the National Technical University "Kharkiv Politechnic Institute", no. 47 (1089), pp. 28–42, 2014. Available: http://nbuv.gov.ua/UJRN/vcpiri_2014_47_7

[12] L. Emelyanov, A. Miroshnikov, I. Domnin, and E. Rogozhkin, "Features of Signals Reception and Processing at the Kharkiv Incoherent Scatter Radar", 2018 International Conference on Information and Telecommunication Technologies and Radio Electronics (UkrMiCo), September 10–14, Odessa, Ukraine, IEEE Conference Publications, pp. 1–5, 2018. https:// doi.org/10.1109/UkrMiCo43733.2018.9047518

[13] T. Grydeland, C. La Hoz, V. Belyey, and A. Westman, "A procedure to correct the effects of a relative delay between the quadrature components of radar signals at base band", Ann. Geophys., 23, pp. 39–46, 2005. https://doi.org/10.5194/angeo-23-39-2005

[14] O. Bogomaz, A Miroshnikov, and I. Domnin, "Peculiarities of database for Kharkiv incoherent scatter radar" 2017 International Conference on Information and Telecommunication Technologies and Radio Electronics (UkrMiCo,) 11–15 Sept. 2017, Odesa, Ukraine, IEEE Conference Publications, pp. 1–4, 2017. https://doi.org/10.1109/UkrMiCo.2017.8095424

[15] I.F Domnin, L.Ya Emelyanov, and L.F. Chernogor, "Dynamics of the ionospheric plasma above Kharkiv during the January 4, 2011 solar eclipse". Radio Physics and Radio Astronomy. vol. 3, no. 4, pp. 311-324, 2012. https://doi.org/10.1615/RadioPhysicsRadioAstronomy.v3.i4.50

[16] O. Bogomaz, D. Kotov, S. Panasenko, and L. Emelyanov, "Advances in software for analysis of Kharkiv incoherent scatter radar data". 2017 International Conference on Information and Telecommunication Technologies and Radio Electronics (UkrMiCo) 11–15 Sept. 2017, Odesa, Ukraine, IEEE Conference Publications, pp. 1–5, 2017. https://doi.org/10.1109/UkrMico.2017.8095425

[17] L. Ya. Emel'yanov, "Incoherent scatter measurement of the electron density altitude profiles", Geomagnetism and Aeronomy, vol. 42, no. 1, pp. 109–113, 2002. Available: https://researchgate.net/publication/286515265

[18] D. T. Farley, "Incoherent Scatter Correlation Function Measurements", Radio Sci., vol. 4, no. 10, pp. 935–953, 1969. https://doi.org/10.1029/RS004i010p00935

[19] L. Ya. Yemelyanov, "Development of principles and instrumentation for generation of test and control signals of the incoherent scatter radar", Telecommunications and Radio Engineering, vol. 76, iss. 14, pp. 1259–1271, 2017. https://doi.org/10.1615/TelecomRadEng.v76.i14.50.